Kharazmi University

Nova Biologica Reperta

Print ISSN: 2423-6330
Online ISSN: 2476-7115

Homepage: https://nbr.khu.ac.ir/

Expression, purification, structure and stability of recombinant bFGF from *E.coli*: A spectroscopic and calorimetry study

Faezeh Ranjbar[1], Nikoo Nasoohi[2]✉, Khosro Khajeh[3]

1. Department of Microbial Biotechnology, Faculty of Advanced Sciences and Technology, Tehran Medical Sciences, Islamic Azad University, Tehran, Iran. E-mail: f76.ranjbar@gmail.com
2. Department of Molecular and Cellular Sciences, Faculty of Advanced Sciences and Technology, Pharmaceutical Sciences Branch, Islamic Azad University (IAUPS), Tehran, Iran. E-mail: nikoo_nasoohi@yahoo.com
3. Department of Biochemistry, faculty of Biological sciences, Tarbiat Modares University, Tehran, Iran. E-mail: khajeh@modares.ac.ir

Article Info

Article type:
Research Article

Article history:
Received 6 April 2025
Received in revised form 17 May 2025
Accepted 3 June 2025
Available online - - 2025

Keywords:
Basic fibroblast growth factor,
Wound healing,
nanoparticle,
purification,
Protein's structure and stability-Biophysical approaches

ABSTRACT

Objective: Basic fibroblast growth factor (bFGF), also known as FGF-2, is a crucial member of the fibroblast growth factor family, involved in a variety of biological functions including cellular proliferation, wound healing, angiogenesis, intercellular signalling, and cell differentiation, In contemporary stem cell research, serum-free media enriched with various additives and growth factors are employed, and among these, bFGF being particularly significant. Despite its extensive potential applications, the clinical utilization of bFGF is limited due to its instability, especially in aqueous environment. Therefore, a thorough investigation of the protein's structural integrity and stability is essential. This study focuses on the expression, purification, and characterization of bFGF for structural and stability analysis through biophysical methods.

Method: The differential scanning calorimetry (DSC) used for stability analysis. Furthermore, the study aims to evaluate the biological activity of the protein in cellular context. For this purpose, gold nanoparticles were synthesized.

Results: The results from the Cell Migration Assay indicated that the proliferation of HT29 cells was enhanced following treatment with bFGF in conjunction with gold nanoparticles. Also, a MTT assay was conducted.

Conclusions: Intrinsic fluorescence measurement indicated a structural alteration surrounding the tryptophan residue, while circular dichroism (CD) analysis showed a decrease in the protein's secondary structure.

Cite this article: Ranjbar, F., Nasoohi, N., & Khajeh, Kh. (2025). Expression, purification, structure and stability of recombinant bFGF from *E.coli*: A spectroscopic and calorimetry study. *Nova Biologica Reperta*, *12*(2), 1-20. http//doi.org/10.22034/NBR.12.2.2

Publisher: Kharazmi University.
DOI: http//doi.org/10.22034/NBR.12.2.2

[DOI: 10.22034/NBR.12.2.2]

Introduction

The mammalian fibroblast growth factor (FGF) family is composed of 18 glycoproteins that are secreted and activated by FGF receptors (FGFRs), playing essential roles throughout both developmental and adult life stages. In the context of development, FGFs and FGFRs are pivotal in the regulation of mesodermal patterning and organ formation. In adult organisms, these molecules are involved in the regulation of numerous processes related to angiogenesis, including the mechanisms of wound healing (1). Fibroblast growth factors exhibit extensive mitogenic activity, stimulating growth in fibroblasts, malignant cells, and endothelial cells. Furthermore, FGFs are vital for the maintenance of adult organ systems, tissue regeneration, hematopoiesis, and embryonic development (2). The identified protein family can be categorized into two main types: FGF1 (aFGF) and FGF2 (bFGF). The endogenous protein bFGF, which has a molecular weight of 18 kDa and binds heparin, is recognized for its ability to enhance cell migration, proliferation, and differentiation across various tissues (3).

The crystallographic analysis of FGF2 reveals that the protein has a globular conformation, with a folded diameter of around 4 nanometers. Its tertiary structure is defined by a β barrel, which consists of 12 antiparallel β strands interconnected by β turns (4). A multitude of clinical trials has recognized and evaluated the diverse therapeutic uses of bFGF, encompassing the treatment of diverse medical conditions such as burns, oral ulcers, fractures, pressure and diabetic ulcers (3), and ischemic brain injuries (5).

The stability of the bFGF protein is a significant concern in its application for the development of pharmaceutical products, a fact that is broadly recognized in the field (4) . Circular dichroism (CD) is a reliable method extensively employed for the analysis of various protein structures and their stability (6,7,8,9). Conversely the fluorescence technique serves as a highly informative tool in the investigation of protein conformational changes, offering significant insights into protein chemistry and biophysics. This is achieved through the phenomenon of emission maximum shift, which can be effectively integrated with quenching and self-quenching processes (9,10,11,12). The present investigation aims to produce the bFGF protein and improve protein expression in E. coli bacteria. Additionally, this study pursues performing structural and stability studies on the protein through circular dichroism (CD) and intrinsic fluorescence spectroscopy approaches. This study investigates protein activity in the context of gold nanoparticles, examining their effects through wound healing repair tests and MTT assays, both in their presence and absence. Differential scanning calorimetry (DSC) is widely recognized as a valuable technique for assessing the equilibrium thermodynamic stability and stability mechanisms of proteins. Additionally, it can be employed qualitatively to evaluate thermal stability, which serves as an indicator of ligand binding. There are numerous documented instances of its application in this context (13,14). The final step involves the validation of the thermodynamic parameters using the DSC technique. The documents from various studies suggest that gold nanoparticles significantly enhance the cell proliferation

[DOI: 10.22034/NBR.12.2.2]

effects of bFGF and also have a notable impact on reducing the cytotoxicity of bFGF which completely aligne with our study (15, 16, 17).

Method

The fibroblast growth factor 2 gene was inserted into the pET-21a construct. This gene features a hexa-His tag at the C-terminus and is responsible for producing wild-type bFGF. The chemicals and reagents utilized in this study, along with the dialysis tubing's cellulose membrane, were sourced from Sigma-Aldrich. Additionally, the LB medium and kanamycin sulfate required for bacterial culture were also obtained from Sigma-Aldrich. IPTG and the E. coli BL21 DE3 strain were acquired from Thermo Fisher. RPMI-1640 culture medium, fetal bovine serum, trypsin, as well as penicillin and streptomycin antibiotics, were provided by Gibco. The HT29 cell line was procured from the cell bank of the Iran Pasteur Institute.

1.1 Protein expression and purification

The gene responsible for encoding fibroblast growth factor 2, appended with a HisTag at the N-terminal, was cloned into the NdeI and XhoI restriction sites of the pET-21a vector. Following this, the plasmid was introduced into the E. coli BL21 (DE3) expression strain, and the resulting colony was cultured in LB media supplemented with 100 mg/mL of ampicillin. The bacterial culture was incubated at 37 °C with shaking at 180 rpm until the optical density at 600 nm (OD600) reached 0.5. At this point, isopropyl β-D-1-thiogalactopyranoside (IPTG) was added to a final concentration of 1 mM to induce protein expression, and the culture was maintained at 37 °C for an additional 4 hours. Subsequently, the bacterial cells containing the recombinant protein were harvested by centrifugation at 4000 RPM at 4 °C, and the resulting pellet was collected. To facilitate cell lysis, a lysis buffer composed of 50 mM Tris-HCl, 1 mM phenylmethylsulfonyl fluoride (PMSF), 300 mM NaCl, 10 mM imidazole, and a protease inhibitor cocktail was prepared at pH 8. The bacterial pellet was then resuspended in this lysis buffer, and the mixture was subjected to intense sonication for 10 minutes while kept on ice. Finally, the sample underwent centrifugation at 12000 RPM to separate the pellet from the supernatant, and the presence of proteins in the supernatant was confirmed using SDS-PAGE with a 12.5% gel.

The Ni-NTA affinity chromatography technique was employed owing to the presence of a 6-histidine tag at the N-terminus of the target protein. Initially, the resin was equilibrated using 10 ml of the lysis buffer obtained from the previous step. Subsequently, 5 ml of the supernatant was introduced into the column, which was then placed on a rotator for one hour to ensure gentle mixing. Following this, wash steps were conducted by incrementally increasing the imidazole concentration to 20 mM and 40 mM, each with a volume of 10 ml. After confirming the absence of absorption through UV detection at 280 nm, the target protein was eluted using a solution of 300 mM imidazole.

[DOI: 10.22034/NBR.12.2.2]

1.2 Determination of protein concentration by Bradford method

After dissolving 100 mg of Coomassie Brilliant Blue G-250 powder in 5 mL of 96% ethanol and adding 100 mL of 85% phosphoric acid (w/v), a solution was prepared. The final volume of the resulting solution was brought up to one liter with distilled water and filtered using filter paper.

1.2.1 Protein Standard Solution

A BSA (Bovine Serum Albumin) solution with a concentration of 1 mg/mL was used to prepare the standard. The absorbance of the resulting sample contents from the tubes was read at a wavelength of 595 nm after 15 minutes of mixing. Finally, the concentration of the unknown protein was determined.

After purification, the eluted samples were collected in three stages, and their absorbance was measured at 280 nm using an ELISA reader. Then, their concentration was determined using the Bradford method

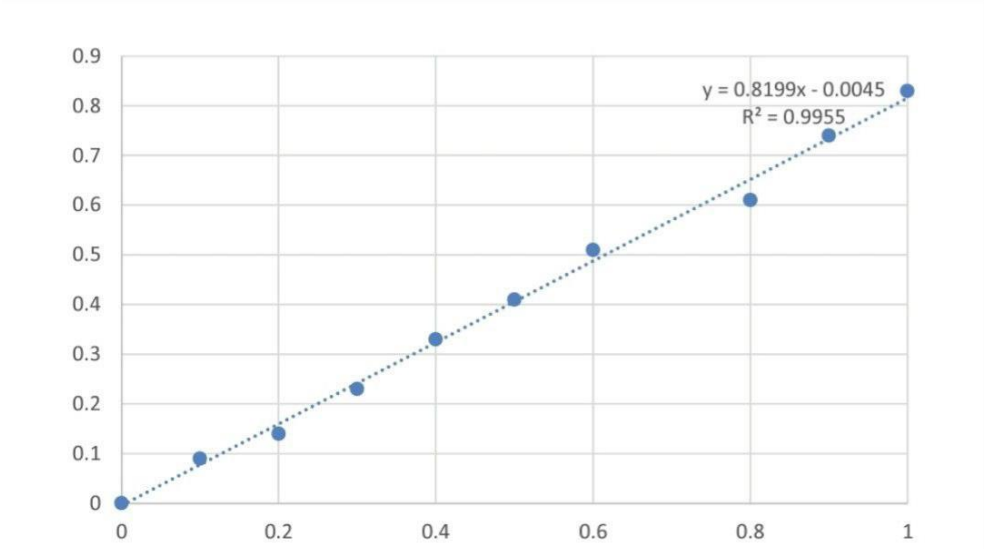

Fig. 1. Bradford Calibration Curve for Determining Protein Concentration

To eliminate excess imidazole, which adversely affects spectroscopic analyses and poses toxicity to cells in cellular studies, we utilized a dialysis technique. Initially, the dialysis bag tube was regenerated, followed by the introduction of 0.8 mg/ml of pure bFGF into the bag (flat width: 29 mm; MWCO: 14.5 kD). The dialysis process was carried out overnight at 4°C, utilizing a buffer composed of 50 mM Tris-HCl and 100 mM NaCl, adjusted to a pH of 7.

1.3 Synthesis of gold nanoparticles and interaction with bFGF

A total of 500 microliters of a gold solution with a concentration of 0.01 M was combined with 19.5 milliliters of double-distilled water and heated until boiling. Following this, 600

[DOI: 10.22034/NBR.12.2.2]

microliters of 0.16 M sodium nitrate were introduced into the mixture, which was then maintained at 70°C for a duration of 15 minutes. After synthesis, the nanoparticles were characterized using transmission electron microscopy (TEM) after cooling and storing them at 4°C in a refrigerator.

Using bFGF protein at a concentration of 0.01 mg/mL (equivalent to 60 ng/mL) and gold nanoparticles synthesized at a concentration of 2.28×10^{-7} M, a final concentration of 50 ng/mL is prepared. Ultimately, an interaction is carried out between the protein and the synthesized gold nanoparticles using the specified concentrations.

To achieve this, 200 µL of bFGF protein is diluted with double-distilled water to a final volume of 1 mL, resulting in a concentration of 200 ng/mL. This dilution is necessary to account for the expected dilution of the protein upon mixing with the culture medium.

Similarly, for the synthesized gold nanoparticles, 440 µL of the nanoparticle solution is diluted with 560 µL of double-distilled water to reach a concentration of 150 ng/mL, which will then be diluted to 50 ng/mL after mixing with the culture medium.

For the interaction between the protein and gold nanoparticles, 440 µL of the nanoparticle solution is mixed with 200 µL of protein solution and 360 µL of double-distilled water, resulting in final concentrations of 200 ng/mL for the protein and 150 ng/mL for the gold nanoparticles. These will then be further diluted to the desired concentrations upon addition to the culture medium.

1.4 Intrinsic protein fluorescence study in the presence of 8 M urea.

In this study, bFGF protein was employed at a concentration of 0.02 mg/ml, with aromatic residues being excited at a wavelength of 280 nm. The intrinsic fluorescence intensity of the pure protein was measured within an emission range of 300 to 500 nm. The bFGF was subjected to titration with 8 M urea, maintaining an equivalent volume ratio, and the dilution factor was incorporated into the concentration calculations. The scanning rate was set at 1000 nm/m, and both the excitation and emission slit widths were fixed at 5 nm. A Perkin Elmer fluorimeter LS 55 (PerkinElmer, USA) was utilized to assess the structural changes of bFGF based on its intrinsic fluorescence emission.

1.5 Circular dichroism spectropolarimeter

To examine the content of the secondary structure, circular dichroism (CD) measurements were conducted in the far ultraviolet region, specifically between 200 and 250 nm. This study was conducted in a 1-mm path-length cuvette using a JASCO J-715 CD spectropolarimeter (Tokyo, Japan). The present study is based on a protein concentration of 0.2 mg/ml. The parameter of ellipticity was normalized using the formula $[\theta]= \theta \times 100MRW/(C \times l)$, that θ refers to ellipticity measured by spectropolarimeter in degree at wavelength of λ, MRW is mean amino acid residue weight, C refers to sample concentration and l is the length of the cuvette cell.

[DOI: 10.22034/NBR.12.2.2]

1.6 Structural Stability Assessment of BFGF via Urea Titration.

For this examination, concentrations of 0.2 mg/ml were used for both intrinsic fluorescence emission and circular dichroism spectra, respectively. Regarding the minor conformational alteration in our evaluation, a large volume of protein was employed. For the CD analysis, a sigmoid curve was generated using θ=222, which was informed by the detection of notable changes in the content of α-helixes. Additionally, to identify the critical regions of the graph, urea was employed as a chemical denaturant, with concentrations varying from 0.5 to 8 M.

1.7 Differential scanning calorimetry (DSC) evaluation.

In the present investigation, a concentration of 0.16 mg/ml was chosen, and the corresponding thermogram was obtained over a temperature range of 20 to 90 °C. The variations in heat capacity at constant pressure were graphed as a function of temperature. The Nano DSC III (USA TA instrument) was utilized for this purpose.

1.8 Cell viability assay.

The cytotoxicity of basic fibroblast growth factor (bFGF) was assessed in both the presence and absence of gold nanoparticles (AuNP) using the MTT assay. In this context, we investigated the independent effects of bFGF as well as the interaction between AuNP and bFGF on the viability of HT29 cell lines. The experiments utilized bFGF at a concentration of 60 ng/ml, both alone and in conjunction with AuNP at 50 ng/ml, over incubation periods of 24, 48, and 72 hours. Initially, 5×10^3 cells were plated in each well of 96-well plates and allowed to reach confluence overnight. Subsequently, the old culture medium was discarded and replaced with fresh medium. After a 48-hour period, 5 mg/ml of MTT solution was introduced to the wells. After 4 hours, the MTT solution was discarded, and 150 microliters of DMSO were used to dissolve the precipitated crystals. The decrease in absorption of MTT was subsequently measured at 570 and 630 nm utilizing ELISA Reader.

1.9 Wound Healing assay.

This test examined the effects of bFGF independently and in interaction with gold nanoparticles on the migration and proliferation of the HT29 cells. The concentrations of bFGF and AuNP utilized in the study were 60 ng/ml and 50 ng/ml, respectively. For all assessments, HT29 cells were cultured in 12-well plates and maintained in RPMI supplemented with 10% fetal bovine serum (FBS) at a temperature of 37°C and a carbon dioxide concentration of 5% for durations of 24, 48, and 72 hours. Upon reaching approximately 70% confluence, two separate regions of the HT29 cell monolayer at the bottom of each well were subjected to scratching using a sterile pipette tip with a volume range of 10–100 microliters. The growth of cells on either side of the scratch towards the center was quantified using ImageJ software.

[DOI: 10.22034/NBR.12.2.2]

HT29 cells were grown in the (RPMI 1640) containing 10% Fetal Bovine Serum and 40 mg/mL of penicillin-streptomycin. The cells were grown to 70% confluence with daily medium changes. All cells grew at 37°C, 5% of CO2, and in a humidified incubator.

1.10 Statistical analysis.

The results were all represented as means±SE of three distinct experiments. A one way ANOVA analysis of variance was used to look for statistical variations in the datasets; a P-value of 0.05 was regarded as significant.

Results

1.1 Protein expression and purification

A suitable purification protocol was implemented based on the expression of the soluble bfGF protein in E. coli. It is important to highlight that not all recombinant proteins were present in the supernatant; some were found as inclusion bodies resulting from bacterial overexpression. Nonetheless, the achieved expression level and the subsequent purification were adequate to advance our systematic biophysical investigation.

1.2 Bio-thermodynamic evaluation, and cell biology studies.

A pure protein as depicted in Figure 1, exhibits a molecular weight of roughly 35 kilodaltons when analyzed via SDS-PAGE. It is important to note that the Bradford assay was employed to assess protein concentration consistently throughout the study.

[DOI: 10.22034/NBR.12.2.2]

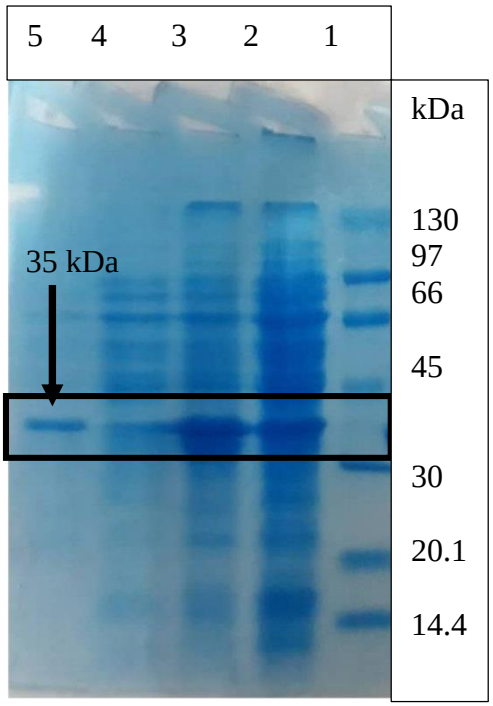

Fig. 2. SDS-PAGE 12.5%: 1.Protein Marker, 2.protein crude in the supernatant, 3.cell pellet, 4.BL21 Negative Control, and 5.Purified Band (35 kDa), in order from right to left, are shown on the gel.

1.3 Protein stability utilizing Intrinsic fluorescence spectroscopy

Figure 2 illustrates a decline in fluorescence emission, indicating that the bFGF protein progressively loses its structural rigidity during the urea titration process. Tryptophan, the key aromatic residue involved in these changes, plays a crucial role, with the surrounding environment contributing significantly to the structural modifications observed during denaturation, particularly when excitation is performed at 280 nm.

[DOI: 10.22034/NBR.12.2.2]

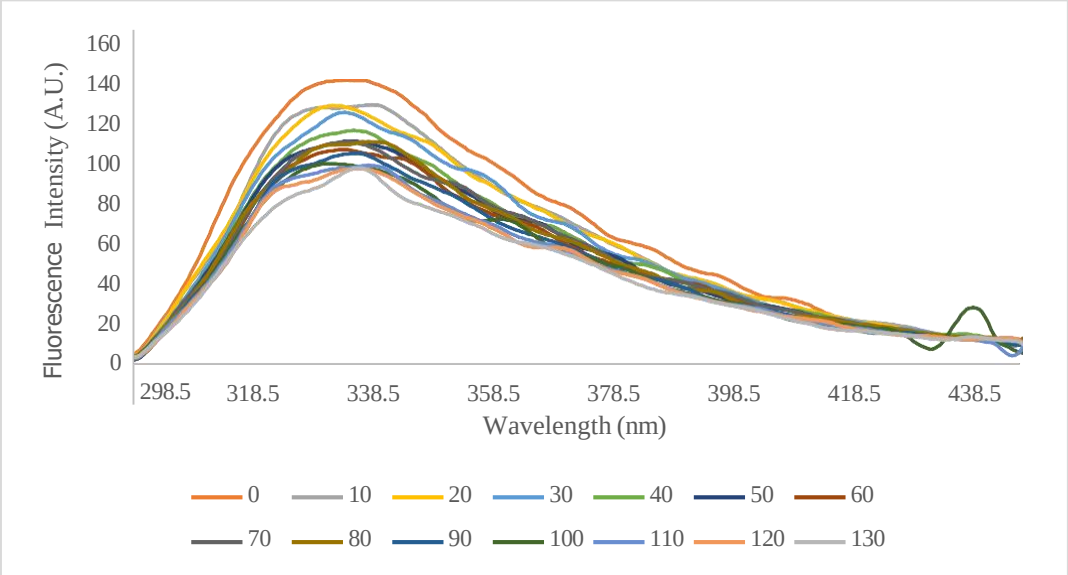

Fig. 3. Intrinsic fluorescence spectra of the bFGF protein in absence and presence of different concentrations of urea. (in which 10-130 equals to 0.27-3.5 M of urea)

1.4 Looking into bFGF protein chemical stability employing circular dichroism

In this investigation, it was observed that a predominant number of the structures exhibited the alpha+ beta motif, although the corresponding data were not presented. The titration process with urea, illustrated in Figure 3A, revealed a decrease in the proportion of secondary structural content. For the comprehensive validation assessment, alterations in molecular ellipticity obtained from circular dichroism (CD) at a wavelength of 222 nm were plotted against varying concentrations of urea, revealing two-state transitions between the native and denatured forms, as depicted in the sigmoid curve shown in Figure 3B. The Gibbs free energy equation was employed to evaluate protein stability, yielding a value of 1.090 kJ/mol, which suggests a low level of protein stability.

[DOI: 10.22034/NBR.12.2.2]

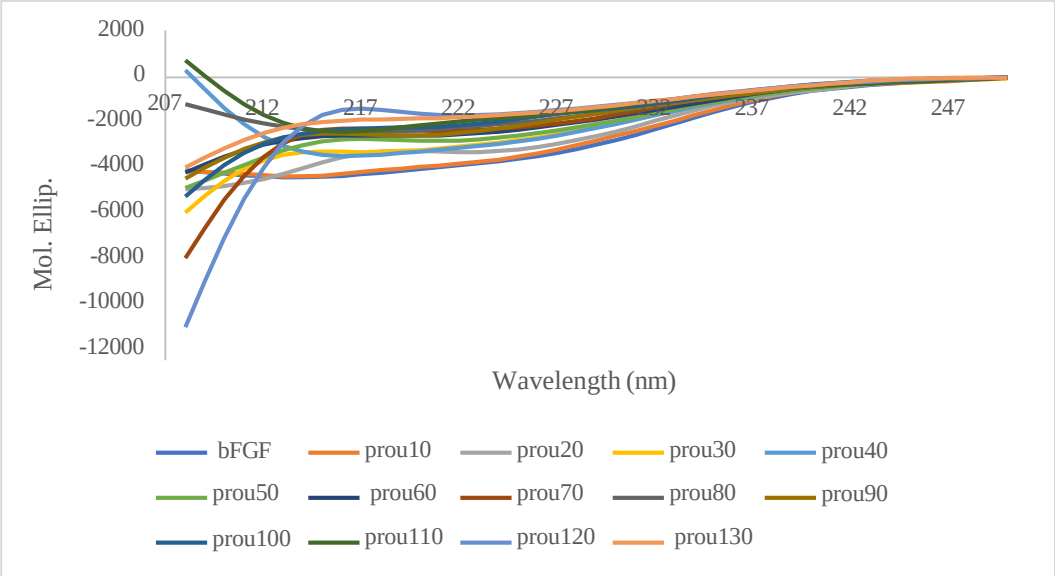

Fig. 4A. Far-UV CD spectra of bFGF at various urea concentrations. (in which 10-130 equals to 0.27-3.5 M of urea)

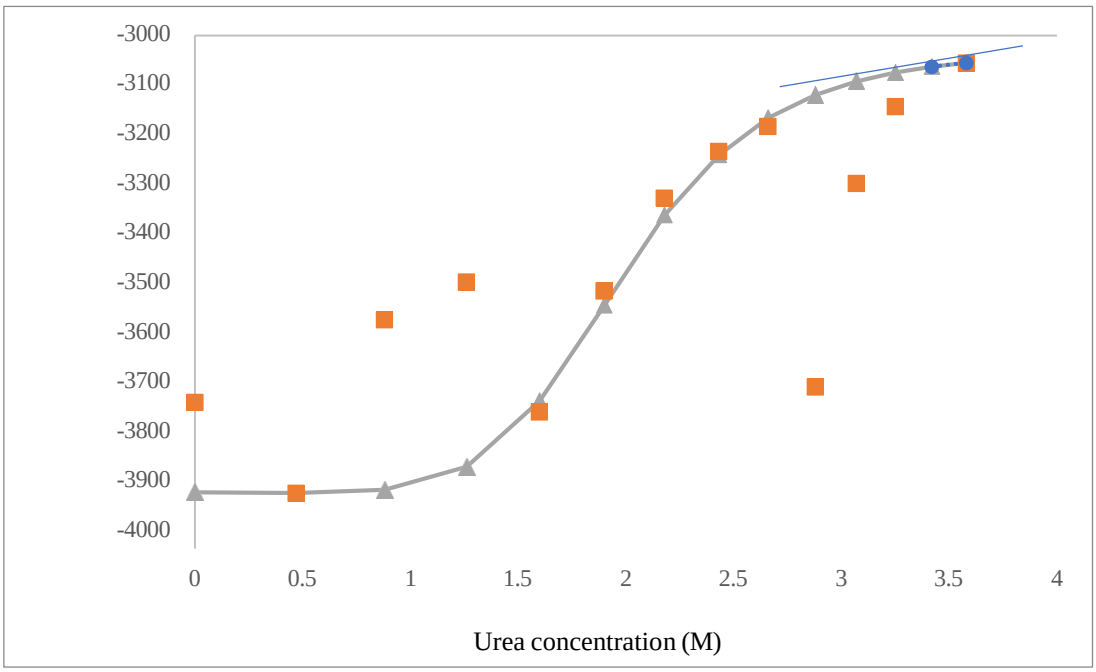

Fig. 4B. The changes in molar ellipticity at 222 nm versus varied urea concentrations followed a sigmoidal trend.

[DOI: 10.22034/NBR.12.2.2]

1.5 Differential scanning calorimetry results

The Cp baselines for both the native and denatured states of bFGF indicate that the protein remains non-aggregated, and the denaturation process is reversible within the specified temperature range, as illustrated in Figure 4. The thermogram obtained from the experiment demonstrated a melting temperature (Tm) of 50.14 °C. Further analysis of this thermogram yielded enthalpy and entropy values of 17.440 kJ/mol and 0.0539 kJ/mol, respectively. Using the Gibbs free energy equation, we calculated ΔG to be 1.37 kJ/mol. Importantly, a temperature of 25 °C serves as a reliable indicator of protein stability.

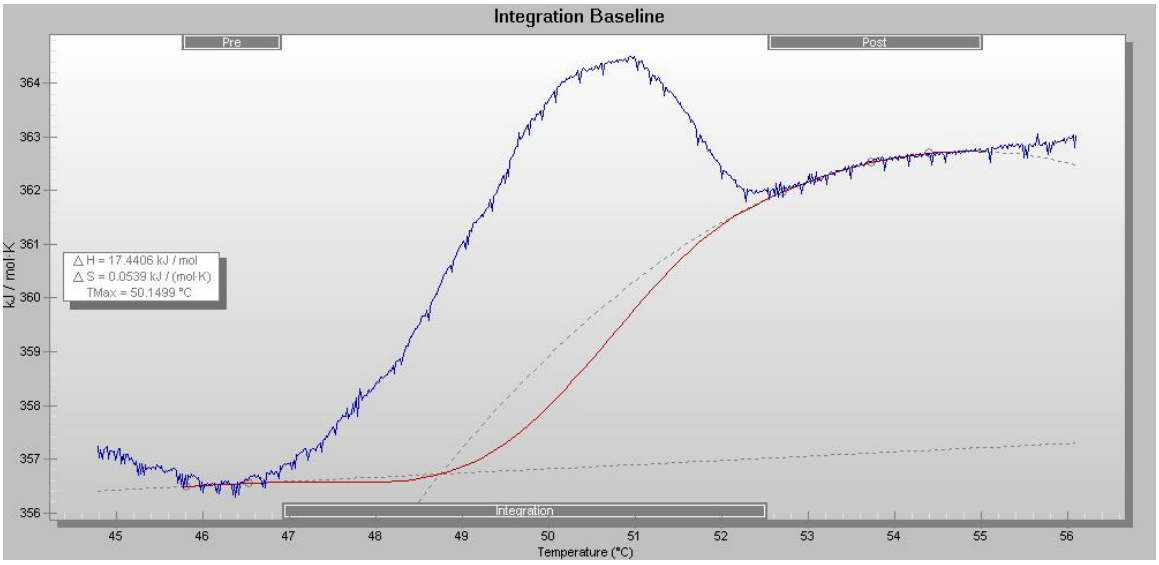

Fig. 5. The calorimetrically measured partial molar heat capacity profile of bFGF.

1.6 Cell migration assay results

The influence of gold nanoparticles on cell growth has been previously established; therefore, a cell scratch assay was employed to assess the effects of bFGF on the proliferation and migration of HT29 cells. To explore the combined effects of nanoparticles and proteins through their interactions, treatments were administered over 24, 48, and 72 hours. As illustrated in Figure 5A, after 72 hours, HT29 cells treated with bFGF displayed significant growth and regenerative characteristics. In Figure 5B, the synergistic effect of bFGF and gold nanoparticles demonstrates that, compared to proteins independently, the proliferation of HT29 cells is accelerated when gold nanoparticles and bFGF interact.

[DOI: 10.22034/NBR.12.2.2]

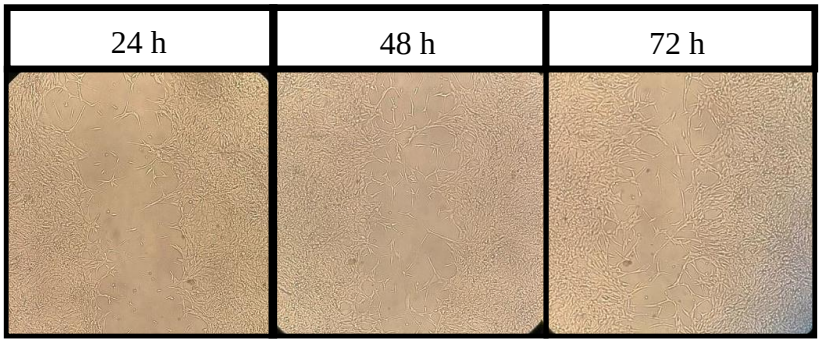

Fig. 6A. The outcomes of cell migration after treatment with bFGF protein over time show a clear progression upward. Magnification: ×100

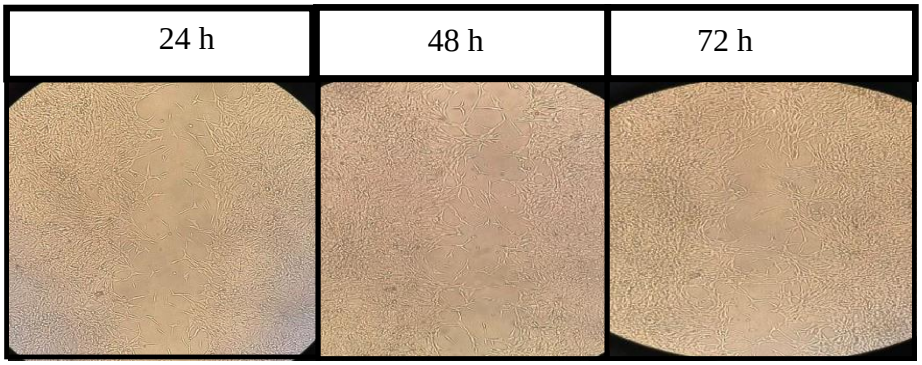

Fig. 6B. The collaborative impact of gold nanoparticles' interaction with the bFGF protein on cell migration increased with time. Magnification: ×100

1.7 MTT assay results

The purpose of this experiment was to determine the cellular toxicity of bFGF protein in the presence and absence of gold nanoparticles. The HT29 cell line underwent treatment with bFGF protein, gold nanoparticles, and a combination of bFGF protein with gold nanoparticles for durations of 24, 48, and 72 hours, resulting in three distinct experimental groups. The findings demonstrated that cell death is influenced by the duration of exposure, with variations in cell viability observed over time. Additionally, the presence of gold nanoparticles enhanced the effects of the bFGF protein.

[DOI: 10.22034/NBR.12.2.2]

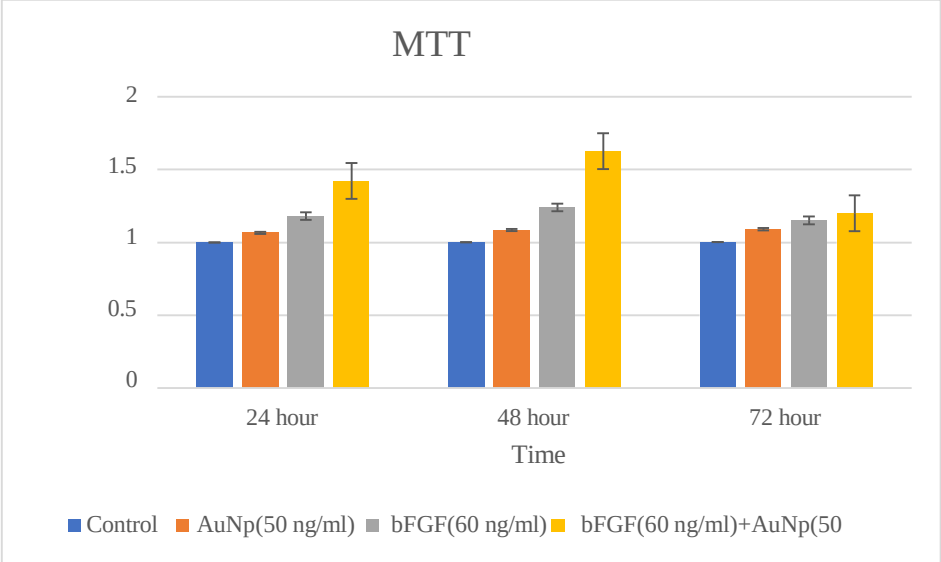

Fig. 7. Each column represents the effect of the group being tested on the percentage of time-dependent cell proliferation, while each error bar reflects the standard deviation.

Conclusions

In most prior studies examining the structure and function of basic fibroblast growth factor (bFGF), various chromatography techniques, particularly those utilizing fast protein liquid chromatography (FPLC) and high-performance liquid chromatography (HPLC), were employed. However, in the present study, we adopted a straightforward and economical method utilizing nickel affinity chromatography. We implemented a batch-gravity approach, and the findings demonstrated that this technique produces comparable results for laboratory-scale experiments, although it is not appropriate for industrial applications.(18, 19) Previous literature has demonstrated that Ni-NTA chromatography can produce comparable results to automated systems for His-tagged proteins under optimized conditions. Moreover, the documents depicted that this technique is cost effective and suitable for laboratory scale studies. Which exactly align with our experiment situation and results.(20, 21, 22, 23)

The data presented in Figure 2 illustrates a reduction in the intrinsic fluorescence intensity of bFGF when exposed to varying concentrations of urea. This observation suggests a decrease in the rigidity of the protein structure surrounding the tryptophan residue. Furthermore, Figure 3A depicts the circular dichroism spectrum of bFGF across different urea concentrations, indicating that an increase in urea concentration correlates with a reduction in structural compaction. To assess the stability of this protein at ambient temperature, the θ_{222} value was plotted against urea concentration, as shown in Figure 3B. The resulting sigmoid curve allowed

[DOI: 10.22034/NBR.12.2.2]

for the calculation of the ΔG parameter, which was determined to be 1.090 kJ, indicating that bFGF exhibits lower stability in comparison to other proteins within the same family.(24, 25, 26)

To reveal the effect of ΔG obtained from CD spectroscopy, the stability of the protein was investigated by DSC method, and the DSC thermogram of this protein was plotted against the temperature, which can be seen in Figure 4, shows how the changes in specific heat capacity at constant pressure in different temperatures cause denaturation changes between the two states. According to the baselines of C_P^N and C_P^D, aggregation was not observed and the thermogram was reversible, and the values of ΔH and ΔS were 4406.17 kJ/mol and 0.0539 kJ/mol, respectively, and through the formula $\Delta G = \Delta H - T\Delta S$, the value of ΔG was calculated equal to 1.37 kJ/mol, which confirms the value of ΔG by CD method. (13, 27, 28, 29, 30)

The non-cytotoxic nature of these nanoparticles has been well-documented in numerous studies, which have explored the dose-dependent effects of gold nanoparticles in various geometries, including rod, spherical, tubular, and star shapes, on different cell lines. Given the susceptibility of the bFGF protein to proteolysis, this study aimed to assess not only whether gold nanoparticles enhanced the protein's effects synergistically but also to investigate the interactions between these two components during cellular analysis. Furthermore, the presence of gold nanoparticles significantly reduced the cytotoxic effects of bFGF, as evidenced by a comparison with conditions lacking these nanoparticles. (31, 19, 32, 33, 34, 35)

Author Contributions

Kh.Kh. obtained the funding and conceived the idea. F.R. conducted the experiments. F.R., N.N. wrote the paper. All authors analysed the results and reviewed the manuscript.

Data Availability Statement

The authors declare that the data supporting the findings of this research are available within the article.

Acknowledgements

The authors would like to thank the research council of Islamic Azad University and Tarbiat Modares University for the financial support of this investigation. And also would like to thank Dr. Saeed Hesami Tackallou and Milad Amiri for editing of the paper, Dr. Reza Hassan Sajedi for his consultation.

Ethical Considerations

No In vivo experiments were conducted in this study.

[DOI: 10.22034/NBR.12.2.2]

Funding

This study was self-funded.

Conflict of Interest

The authors declare no conflict of interest.

[DOI: 10.22034/NBR.12.2.2]

References

1. Zahra FT, Sajib MS, Mikelis CM. Role of bFGF in acquired resistance upon anti-VEGF therapy in cancer. Cancers. 2021 Mar 20;13(6):1422. https://doi.org/10.3390/cancers13061422
2. Akl MR, Nagpal P, Ayoub NM, Tai B, Prabhu SA, Capac CM, Gliksman M, Goy A, Suh KS. Molecular and clinical significance of fibroblast growth factor 2 (FGF2/bFGF) in malignancies of solid and hematological cancers for personalized therapies. Oncotarget. 2016 Mar 19;7(28):44735. https://doi.org/10.18632/oncotarget.8203
3. Benington LR, Rajan G, Locher C, Lim LY. Stabilisation of recombinant human basic fibroblast growth factor (FGF-2) against stressors encountered in medicinal product processing and evaluation. Pharmaceutics. 2021 Oct 21;13(11):1762. https://doi.org/10.3390/pharmaceutics13111762
4. Benington L, Rajan G, Locher C, Lim LY. Fibroblast growth factor 2—A review of stabilisation approaches for clinical applications. Pharmaceutics. 2020 Jun 2;12(6):508. https://doi.org/10.3390/pharmaceutics12060508
5. Mu X, Kong N, Chen W, Zhang T, Shen M, Yan W. High-level expression, purification, and characterization of recombinant human basic fibroblast growth factor in Pichia pastoris. Protein expression and purification. 2008 Jun 1;59(2):282-8. https://doi.org/10.1016/j.pep.2008.02.009
6. Maroufi B, Ranjbar B, Khajeh K, Naderi-Manesh H, Yaghoubi H. Structural studies of hen egg-white lysozyme dimer: Comparison with monomer. Biochimica et Biophysica Acta (BBA)-Proteins and Proteomics. 2008 Jul 1;1784(7-8):1043-9. https://doi.org/10.1016/j.bbapap.2008.03.010
7. Saboury AA, Karbassi F, Haghbeen K, Ranjbar B, Moosavi-Movahedi AA, Farzami B. Stability, structural and suicide inactivation changes of mushroom tyrosinase after acetylation by N-acetylimidazole. International journal of biological macromolecules. 2004 Aug 1;34(4):257-62. https://doi.org/10.1016/j.ijbiomac.2004.06.003
8. Ganjalikhany MR, Ranjbar B, Hosseinkhani S, Khalifeh K, Hassani L. Roles of trehalose and magnesium sulfate on structural and functional stability of firefly luciferase. Journal of Molecular Catalysis B: Enzymatic. 2010 Feb 1;62(2):127-32. https://doi.org/10.1016/j.molcatb.2009.09.015
9. Miroliaei M, Ranjbar B, Naderi-Manesh H, Nemat-Gorgani M. Thermal denaturation of yeast alcohol dehydrogenase and protection of secondary and tertiary structural changes by sugars: CD and fluorescence studies. Enzyme and microbial technology. 2007 Mar 5;40(4):896-901. https://doi.org/10.1016/j.enzmictec.2006.07.004
10. Farahani N, Behmanesh M, Ranjbar B. Evaluation of Rationally Designed Label-free Stem-loop DNA Probe Opening in the Presence of miR-21 by Circular Dichroism and Fluorescence Techniques. Scientific reports. 2020 Mar 4;10(1):4018. https://doi.org/10.1038/s41598-020-60157-5
11. Gill P, Ranjbar B, Saber R, Khajeh K, Mohammadian M. Biomolecular and structural analyses of cauliflower-like DNAs by ultraviolet, circular dichroism, and fluorescence spectroscopies in comparison with natural DNA. Journal of Biomolecular Techniques: JBT. 2011 Jul;22(2):60.
12. Mehrabi F, Ranjbar B, Hosseini M, Sadeghi N, Mohammadi J, Ganjali MR. CRET-based immunoassay on magnetic beads for selective and sensitive detection of Nanog antigen as a key cancer stem cell marker. Microchimica Acta. 2024 Jul;191(7):419. https://doi.org/10.1007/s00604-024-06505-y

[DOI: 10.22034/NBR.12.2.2]

13. Mohammadi S, Khajeh K, Taghdir M, Ranjbar B. An experimental investigation on the influence of various buffer concentrations, osmolytes and gold nanoparticles on lysozyme: spectroscopic and calorimetric study. International Journal of Biological Macromolecules. 2021 Mar 1;172:162-9. https://doi.org/10.1016/j.ijbiomac.2020.12.208
14. Dabirmanesh B, Daneshjou S, Sepahi AA, Ranjbar B, Khavari-Nejad RA, Gill P, Heydari A, Khajeh K. Effect of ionic liquids on the structure, stability and activity of two related α-amylases. International Journal of Biological Macromolecules. 2011 Jan 1;48(1):93-7. https://doi.org/10.1016/j.ijbiomac.2010.10.001
15. Poomrattanangoon S, Pissuwan D. Gold nanoparticles coated with collagen-I and their wound healing activity in human skin fibroblast cells. Heliyon. 2024 Jul 15;10(13). https://doi.org/10.1016/j.heliyon.2024.e33302
16. Ferreira H, Martins A, da Silva ML, Amorim S, Faria S, Pires RA, Reis RL, Neves NM. The functionalization of natural polymer-coated gold nanoparticles to carry bFGF to promote tissue regeneration. Journal of Materials Chemistry B. 2018;6(14):2104-15. https://doi.org/10.1039/C7TB03273K
17. Vijayan A, Nanditha CK, Kumar GV. ECM-mimicking nanofibrous scaffold enriched with dual growth factor carrying nanoparticles for diabetic wound healing. Nanoscale Advances. 2021;3(11):3085-92. https://doi.org/10.1039/D0NA00926A
18. Wang YJ, Shahrokh Z, Vemuri S, Eberlein G, Beylin I, Busch M. Characterization, stability, and formulations of basic fibroblast growth factor. Formulation, Characterization, and Stability of Protein Drugs: case Histories: case Histories. 2002:141-80. https://doi.org/10.1007/0-306-47452-2_2
19. Sluzky V, Shahrokh Z, Stratton P, Eberlein G, Wang YJ. Chromatographic methods for quantitative analysis of native, denatured, and aggregated basic fibroblast growth factor in solution formulations. Pharmaceutical research. 1994 Apr;11(4):485-90. https://doi.org/10.1023/A:1018946011652
20. Seeger A, Rinas U. Two-step chromatographic procedure for purification of basic fibroblast growth factor from recombinant Escherichia coli and characterization of the equilibrium parameters of adsorption. Journal of Chromatography A. 1996 Oct 4;746(1):17-24. https://doi.org/10.1016/0021-9673(96)00286-5
21. Shahrokh Z, Wang YJ, Stratton PR, Eberlein GA. Approaches to analysis of aggregates and demonstrating mass balance in pharmaceutical protein (basic fibroblast growth factor) formulations. Journal of pharmaceutical sciences. 1994 Dec 1;83(12):1645-50. https://doi.org/10.1002/jps.2600831202
22. Spriestersbach A, Kubicek J, Schäfer F, Block H, Maertens B. Purification of his-tagged proteins. InMethods in enzymology 2015 Jan 1 (Vol. 559, pp. 1-15). Academic Press. https://doi.org/10.1016/bs.mie.2014.11.003
23. Carter TD, Outten FW. Ni-NTA Affinity Chromatography to Characterize Protein–Protein Interactions During Fe-S Cluster Biogenesis. InFe-S Proteins: Methods and Protocols 2021 Jul 23 (pp. 125-136). New York, NY: Springer US. https://doi.org/10.1007/978-1-0716-1605-5_7
24. Longo L, Lee J, Blaber M. Experimental support for the foldability–function tradeoff hypothesis: Segregation of the folding nucleus and functional regions in fibroblast growth factor-1. Protein Science. 2012 Dec;21(12):1911-20. https://doi.org/10.1002/pro.2175
25. Pu F, Wang E, Jiang H, Ren J. Identification of polyoxometalates as inhibitors of basic fibroblast growth factor. Molecular BioSystems. 2013;9(1):113-20. https://doi.org/10.1039/C2MB25389E

[DOI: 10.22034/NBR.12.2.2]

26. Shahrokh Z, Eberlein G, Wang YJ. Probing the conformation of protein (bFGF) precipitates by fluorescence spectroscopy. Journal of pharmaceutical and biomedical analysis. 1994 Aug 1;12(8):1035-41. https://doi.org/10.1016/0731-7085(94)E0030-5
27. Dubey VK, Lee J, Somasundaram T, Blaber S, Blaber M. Spackling the crack: stabilizing human fibroblast growth factor-1 by targeting the N and C terminus β-strand interactions. Journal of molecular biology. 2007 Aug 3;371(1):256-68. https://doi.org/10.1016/j.jmb.2007.05.065
28. Ranjbar B, Gill P. Circular dichroism techniques: biomolecular and nanostructural analyses-a review. Chemical biology & drug design. 2009 Aug;74(2):101-20. https://doi.org/10.1111/j.1747-0285.2009.00847.x
29. Protasevich I, Ranjbar B, Lobachov V, Makarov A, Gilli R, Briand C, Lafitte D, Haiech J. Conformation and thermal denaturation of apocalmodulin: role of electrostatic mutations. Biochemistry. 1997 Feb 25;36(8):2017-24. https://doi.org/10.1021/bi962538g
30. Gill P, Moghadam TT, Ranjbar B. Differential scanning calorimetry techniques: applications in biology and nanoscience. Journal of biomolecular techniques: JBT. 2010 Dec;21(4):167.
31. Tan G, Onur MA. Cellular localization and biological effects of 20nm-gold nanoparticles. Journal of Biomedical Materials Research Part A. 2018 Jun;106(6):1708-21. https://doi.org/10.1002/jbm.a.36373
32. Ferreira H, Martins A, da Silva ML, Amorim S, Faria S, Pires RA, Reis RL, Neves NM. The functionalization of natural polymer-coated gold nanoparticles to carry bFGF to promote tissue regeneration. Journal of Materials Chemistry B. 2018;6(14):2104-15. https://doi.org/10.1039/C7TB03273K
33. Jia X, Tian H, Tang L, Zheng L, Zheng L, Yang T, Yu B, Wang Z, Lin P, Li X, Wang X. High-efficiency expression of TAT-bFGF fusion protein in Escherichia coli and the effect on hypertrophic scar tissue. PloS one. 2015 Feb 23;10(2):e0117448. https://doi.org/10.1371/journal.pone.0117448
34. Tavakoli Z, Ranjbar F, Tackallou SH, Ranjbar B. Nanostructures for the Prevention, Diagnosis, and Treatment of COVID-19: A Review. Particle & Particle Systems Characterization. 2025 Jan;42(1):2400083. https://doi.org/10.1002/ppsc.202400083
35. Yazdanicherati N, Tabarzad M, Daraei B, Ranjbar B. The effect of Pexiganan as an antimicrobial peptide on the structural stability of gold nanoparticles. Modares Journal of Biotechnology. 2024 Feb 10;14(3):0-.

[DOI: 10.22034/NBR.12.2.2]